Received: 4 November 2017 | Revised: 25 January 2018 | Accepted: 25 January 2018

DOI: 10.1111/pce.13160

ORIGINAL ARTICLE

WILEY Plant, Cell & Environment

Hydraulics play an important role in causing low growth rate and dieback of aging *Pinus sylvestris* var. *mongolica* trees in plantations of Northeast China

Yan-Yan Liu[1,2,3] | Ai-Ying Wang[1,2] | Yu-Ning An[4] | Pei-Yong Lian[5] | De-Dong Wu[4] | Jiao-Jun Zhu[1] | Frederick C. Meinzer[6] | Guang-You Hao[1]

[1] CAS Key Laboratory of Forest Ecology and Management, Institute of Applied Ecology, Chinese Academy of Sciences, Shenyang 110164, China

[2] University of Chinese Academy of Sciences, Beijing 100049, China

[3] Key Laboratory of Environment Change and Resources Use in Beibu Gulf, Ministry of Education, Guangxi Teachers Education University, No. 175 Mingxiu East Road, Nanning 530001, China

[4] Institute of Sand Fixation and Silviculture, Liaoning Province, Fuxin 123000, China

[5] Daxinganling Academy of Forest Science of Inner Mongolia, Yakeshi 022150, China

[6] USDA Forest Service, Pacific Northwest Research Station, Corvallis, OR 97331, USA

Correspondence
Guang-You Hao, CAS Key Laboratory of Forest Ecology and Management, Institute of Applied Ecology, Chinese Academy of Sciences, Shenyang 110164, China.
Email: haogy@iae.ac.cn

Funding information
National Natural Science Foundation of China, Grant/Award Numbers: 31722013 and 31500222; National Key Research and Development Program of China, Grant/Award Number: 2016YFA0600803; Project of Natural Science and Technology of Liaoning Province of China, Grant/Award Number: 20170540899; Key Research Project from the Bureau of Frontier Science and Education Chinese Academy of Sciences, Grant/Award Number: QYZDJ-SSW-DQC027; Hundred-Talents Program from the Chinese Academy of Sciences

Abstract

The frequently observed forest decline in water-limited regions may be associated with impaired tree hydraulics, but the precise physiological mechanisms remain poorly understood. We compared hydraulic architecture of Mongolian pine (*Pinus sylvestris* var. *mongolica*) trees of different size classes from a plantation and a natural forest site to test whether greater hydraulic limitation with increasing size plays an important role in tree decline observed in the more water-limited plantation site. We found that trees from plantations overall showed significantly lower stem hydraulic efficiency. More importantly, plantation-grown trees showed significant declines in stem hydraulic conductivity and hydraulic safety margins as well as syndromes of stronger drought stress with increasing size, whereas no such trends were observed at the natural forest site. Most notably, the leaf to sapwood area ratio (LA/SA) showed a strong linear decline with increasing tree size at the plantation site. Although compensatory adjustments in LA/SA may mitigate the effect of increased water stress in larger trees, they may result in greater risk of carbon imbalance, eventually limiting tree growth at the plantation site. Our results provide a potential mechanistic explanation for the widespread decline of Mongolian pine trees in plantations of Northern China.

KEYWORDS

cavitation, embolism, forest decline, hydraulic failure, hydraulic limitation, tree mortality, xylem

1 | INTRODUCTION

Forest decline is widespread across the globe and appears to be accelerating over the past few decades (Allen et al., 2010; Bennett, McDowell, Allen, & Anderson-Teixeira, 2015; Ryan, 2015). Besides natural senescence, tree dieback and mortality result from a combination of biotic and abiotic factors, including damage by insects and pathogens (Wong & Daniels, 2016), nutrient limitation (Xu, McDowell, Sevanto, & Fisher, 2013), and drought stress (Anderegg et al., 2012; Nardini, Battistuzzo, & Savi, 2013; Zheng, Zhu, Yan, & Song, 2012). Due to the influence of climate change, drought has become more frequent and intense in many regions and is becoming

a more and more important factor in causing forest mortality worldwide (Anderegg et al., 2012; Brodribb & Cochard, 2009; Hoffmann, Marchin, Abit, & Lau, 2011; McDowell et al., 2008). Three interactive mechanisms have been proposed to explain tree dieback and mortality in water-limited environments, namely, hydraulic failure, carbon starvation during prolonged stomatal closure, and lethal biotic attacks resulting from climate-mediated insect outbreaks and pathogens (Adams et al., 2009; McDowell et al., 2008; Sevanto, McDowell, Dickman, Pangle, & Pockman, 2014). Although complex reciprocal relationships have been found among the three mechanisms and no single mechanism alone seems to be able to explain widespread tree mortality events, hydraulic failure has been invoked as the most direct mechanism causing tree die-off in vast areas of water-limited land globally, especially under the influence of climate change (Martínez-Vilalta & Piñol, 2002; Nardini et al., 2013; O' Grady, Mitchell, Pinkard, & Tissue, 2013). Nevertheless, knowledge gaps concerning key physiological drivers of tree decline constrain predictions of spatial and temporal patterns of future climate-driven forest die-off (Allen et al., 2010; Balducci, Deslauriers, Giovannelli, Rossi, & Rathgeber, 2013; Hartmann, 2011).

Tree decline has been more frequently observed in larger individuals, and significant changes in hydraulic architecture are also commonly found with increasing tree size, suggesting a mechanistic linkage between mortality and hydraulic limitations mediated by variation in tree size (Woodruff, Meinzer, & Lachenbruch, 2008; Zhang et al., 2009). Water stress is amplified in larger trees due to the negative effects of the gravitational component of water potential and higher resistance associated with a longer hydraulic pathway (Koch, Sillet, Jennings, & Davis, 2004; Ryan, Binkley, & Fownes, 1997). Thus, compared with smaller trees, larger trees might be more susceptible to partial hydraulic failure that leads to lower growth rates, branch dieback, and even mortality (Bennett et al., 2015; Domec et al., 2008; Woodruff, Bond, & Meinzer, 2004). It has been shown that larger trees exhibit more branch damage and greater rates of mortality than co-occurring smaller individuals of the same species in water-limited environments (McDowell & Allen, 2015; Zhang et al., 2009). To avoid the detrimental effects of hydraulic failure, trees may show significant phenotypic plasticity in characteristics related to water transport and use (Domec et al., 2008; Zhang et al., 2009). For example, taller trees of the same species, even growing in a common environment, exhibited greater leaf mass per area, lower leaf area to sapwood area (SA) ratio, lower water potential, lower leaf osmotic potential at full and zero turgor, and lower xylem conductivity (McDowell et al., 2008; Woodruff et al., 2004; Zhang et al., 2009). The mechanisms responsible for the effects of tree size on drought-induced mortality are not fully understood (Martínez-Vilalta, López, Loepfe, & Lloret, 2012; Nardini et al., 2013; Sevanto et al., 2014), and there is an urgent need to study the hydraulic architecture of trees of different sizes to inform predictions of future vulnerability to drought.

Xylem water transport efficiency and safety of trees are strongly influenced by environmental factors and trees have been shown to adjust their hydraulic architecture according to their growing conditions (Magnani, Grace, & Borghetti, 2002; Ryan, Phillips, & Bond, 2006; Schuldt et al., 2016). For example, when grown under xeric conditions at a common site, seedlings of *Pinus pinaster* originating from six populations consistently showed reduced sapwood specific hydraulic conductivity and increased resistance to drought-induced embolism compared with their counterparts growing in a mesic common site (Corcuera, Cochard, Pelegrín, & Notivol, 2011). In spite of the phenotypic plasticity of hydraulic characteristics, chronic or severe drought stress can cause hydraulic limitation or complete failure of xylem water transport that eventually result in tree dieback and mortality (Davis et al., 2002; Nardini et al., 2013). Aside from drought, hydraulic failure can also be caused by freeze–thaw-induced embolism (Langan, Ewers, & Davis, 1997; Mayr et al., 2014; McCulloh, Johnson, Meinzer, & Lachenbruch, 2011; Sperry & Sullivan, 1992), a risk that especially needs to be considered for evergreen trees growing in high latitude and altitude environments (Charrier et al., 2014; Cochard & Tyree, 1990). Freeze–thaw events can induce substantial xylem embolism in overwintering stems and refilling of winter embolism is strongly influenced by environmental conditions (Breshears et al., 2008; Mayr et al., 2014). For example, conifer trees have been found to repair winter embolism and avoid excessive shoot dieback by absorbing water from fog or snow melting on branch surfaces (Breshears et al., 2008; Burgess & Dawson, 2004; Hacke et al., 2015; Mayr et al., 2014; Sparks, Campbell, & Black, 2001). Previous studies on xylem hydraulics in relation to tree dieback have focused mainly on water stress during the growing season and few studies have considered effects of freeze–thaw events and even fewer have considered both factors (Allen et al., 2010).

Mongolian pine (*Pinus sylvestris* var. *mongolica* Litv.) is the most important tree species used for large-scale afforestation projects in water-limited regions of China (Jiang, Zeng, & Zhu, 1997; Song, Zhu, Yan, Li, & Yu, 2015). This species is well adapted to semiarid environments with deep sandy soils in its natural habitats in the western part of Daxinganling, Inner Mongolia, Northeast China. During the past few decades, more than 700,000 hectares of Mongolian pine plantations have been established in the Three-North (northwest, north, and northeast) region of China especially in places with sandy soils. Mongolian pine plantations provide marvellous ecological, economical, and social benefits locally and at regional scales. However, severe decline in Mongolian pine plantations has occurred since the beginning of 1990s (Jiao, 2001; Zhu, Fan, Zeng, Jiang, & Matsuzaki, 2003). Water deficits are considered to be a key determinant of tree dieback and massive mortality of Mongolian pine trees in plantations of this region (Song, Zhu, Li, & Zhang, 2016; Zhu et al., 2003), but the role of xylem hydraulics in tree mortality has not been examined in this species. In contrast to the obvious decline in plantations, no such phenomenon has been observed in the natural habitats of Mongolian pine trees. In the present study, we compared a natural Mongolian pine forest with a Mongolian pine plantation to investigate whether hydraulic constraints play an important role in the growth decline and dieback observed in larger (DBH > 19 cm, older than 30 years) trees at the plantation site. We hypothesized that size-related decline in growth of the plantation trees would be driven by unfavourable changes in hydraulic architecture and difficulties in maintaining adequate carbon balance with increasing tree size. Specifically, we hypothesized that (a) stem hydraulic conductivity of Mongolian pine trees from the plantations would decrease substantially with increasing tree size, whereas in trees from natural forests, it remains relatively stable with increasing tree size; (b) larger Mongolian pine trees from the plantation site would have reduced capacity for photosynthetic carbon assimilation and reduced growth rates compared with trees from the natural forest site;

(c) plantation grown trees would increasingly exhibit a syndrome of increasing hydraulic limitation and drought stress with the increase of size, characterized by symptoms such as lower leaf water potentials and turgor loss points.

2 | MATERIALS AND METHODS

2.1 | Species and site descriptions

Mongolian pine (*Pinus sylvestris* var. *mongolica*) is a geographical variety of Scots pine (*Pinus sylvestris* L.) that is distributed in Northeast Asia. It has been classified into two ecotypes according to their natural habitats of distribution: an ecotype adapted to mountain habitats and one adapted to fixed sand dunes (Kang, Zhu, Li, & Xu, 2004). The latter ecotype, known as Sandy Land Mongolian Pine (SLMP), is restricted to a forest belt of approximately 200 km in length and 14–20 km in width (47°–49°N, 119°–120°E) in the fixed sand dunes of NE China in its natural conditions (Zhu et al., 2003). Due to its strong tolerance of stressful environments (infertile soil, cold temperature, and drought) and adaptation to deep sandy soils, SLMP has been widely used for sandy land reclamation in vast regions of northern China since the 1950s (Zeng, Jiang, Fan, & Zhu, 1996; Zhu et al., 2003). However, since the early 1990s, SLMP plantations have exhibited severe decline and massive mortality, especially in trees larger than 19 cm diameter at breast height (DBH; Song et al., 2016; Zhu et al., 2003 Table 1). This study was conducted at two pure SLMP sites in NE China. The first site is in the Honghuaerji Natural Reserve of Mongolian Pine Forest (47°36′–48°35′ N, 118°58′–120°32′ E, 878 m alt.), which is located in the heart of the natural forest belt of SLMP. The second site is located at plantations of the Institute of Sand Fixation and Silviculture of Zhanggutai, Zhangwu Country, Liaoning province (42°37′–42°50′ N, 122°11′–122°30′ E, 226.5 m alt.), which is the first place that SLMP was successfully planted and spread to other regions of China.

Both study sites are characterized by deep sandy soil and a semi-arid temperate continental climate with hot, dry summers and cold, windy winters. The mean annual precipitation for the natural site and the plantation site is 344 and 491 mm, respectively. Due to the lower latitude and lower elevation of the plantation site, it has substantially higher temperatures, higher potential evaporation, and much lower humidity and fewer snow cover days than the natural forest site (Figure S1 and Table S1). At each study site, five age classes (10, 20, 30, 40, and 50 years) were selected for physiological measurements related to xylem hydraulics, water relations, and carbon assimilation.

2.2 | Tree age, basal area increment, and branch dieback

We estimated the percentage of damaged branches per tree by counting the number of the dead and living branches in each younger tree crown, or visually estimating the percentage of damaged branches in the crowns of taller trees. Tree ages at the plantation site were estimated using the historical records of the local research institute and were confirmed by counting the number of nodes along the tree trunk, which is relatively easy in this species due to the very regular arrangement of branches on nodes formed each year. The same method was used for tree age determination in the natural forest site. The same two persons made the age determinations at both sites and values were used only when the two independent counts were in agreement. Trees of five size classes were selected according to similar ages and growth conditions. Ten trees per age class in each stand were randomly selected for sampling and physiological measurements. We measured the circumference of the tree trunk at 1.3 m to calculate the DBH in each of the selected trees. Basal area increment (BAI) was then calculated by subtracting basal area of younger age classes from basal area of older age classes and divided by the mean number of years between successive age classes.

2.3 | Stem hydraulic conductivity

During the summer and late winter of 2015, 20–30 branches (approximately 1 m in length) were sampled in two to three stands at both the plantation and the natural forest sites in trees of each of the five size classes. One branch from each of the individuals, whose age and DBH had been previously been determined, was sampled at each stand and thus 20–30 branches per size class at both the plantation and natural forest sites were sampled. At the plantation site, only 20 trees in the largest size class were sampled because there were only two plots containing 50-year-old trees. We sampled 4-year-old branches for all the size classes and 3-year-old stem segments were used for hydraulic conductivity measurements. Branches were collected early in the morning from sun-exposed portions of the crown of healthy trees. The cut ends of the branches were immediately recut (approximately 2 cm removed) under water to remove embolized tracheids. A stem

TABLE 1 Characteristics of forest plots and tree age classes sampled at the two study sites

Site	Age (year)	Number of plots	Total number of individuals sampled	Height (m)	DBH (cm)	Dead branches (%)
Plantation	11–13	3	30	4.2 ± 0.1	7.8 ± 0.0	0
	19–25	3	30	6.5 ± 0.1	14.8 ± 0.1	0
	31–33	3	30	8.6 ± 0.2	18.8 ± 0.1	10
	39–40	3	30	9.9 ± 0.3	21.6 ± 0.1	25
	50	2	20	11.6 ± 0.4	30.5 ± 0.1	34
Natural forest	10	3	30	1.4 ± 0.2	4.2 ± 0.3	0
	20	3	30	4.6 ± 0.2	7.8 ± 0.5	0
	30	3	30	7.3 ± 0.3	14.4 ± 0.5	0
	40	3	30	10.1 ± 0.3	21.7 ± 0.6	5
	50–53	3	30	13.8 ± 0.2	35.1 ± 0.9	4

Note. The height and diameter at breast height (DBH) values are means ±1 *SE*.

segment of about 15 cm in length was then taken from the originally sampled branch under water. Stem segments for hydraulic conductivity measurements were kept under water in a cooler during transport to the laboratory. Upon arrival at the laboratory, samples were put into a refrigerator and kept at 4°C before determination of hydraulic conductivity. Hydraulic measurements for all segments were done within 10 days from sampling and tests in separate sets of samples showed no significant change in conductivity before and after storage tested.

For the native hydraulic conductivity ($K_{h\text{-native}}$) measurements, stem segments approximately 7 cm in length (7–10 mm in diameter) were recut under water in the laboratory. After smoothing both ends of the segments with a sharp razor blade under water, the segments were connected to an apparatus filled with degassed and filtered 20 mM KCl solution. A hydraulic head of 50 cm was used to generate a hydrostatic pressure that drove water flow through the stem segment. Hydraulic conductivity (K_h, kg·m·s^{-1} MPa^{-1}) was calculated as

$$K_h = \frac{J_v}{\Delta P/\Delta L}, \quad (1)$$

where J_v is the flow rate through the stem segment (kg·s^{-1}), and the $\Delta P/\Delta L$ is the pressure gradient across the stem segment (MPa·m^{-1}). All stem hydraulic conductivity measurements were made within a week from sampling and showed no significant change during the storage period.

The sapwood-specific hydraulic conductivity (K_s, kg·m^{-1}·s^{-1}·MPa^{-1}) and the leaf-specific hydraulic conductivity (K_l, kg·m^{-1}·s^{-1}·MPa^{-1}) were calculated as K_h divided by SA and total needle area distal to the segment, respectively. Methyl blue dye was perfused into the branch segment under a hydraulic head of 50 cm. Sapwood area was determined at both ends of the segment and the two values were averaged. Images of the transverse cross-sections of the stained stem were obtained using a scanner, and the area of stained portion was analysed using ImageJ software (US national Institutes of Health, Bethesda, MD, USA). More than 30 needles of each plant were randomly selected and scanned for the determination of projected leaf area. The leaf mass per area for each age class, calculated from these scanned leaves, was used to estimate the total distal needle area (LA) of a branch according to the total needle dry mass. The leaf area to SA ratio (LA/SA) was calculated as LA divided by SA for each branch. Wood density was determined using the same sets of samples for hydraulic conductivity measurements by the water displacement method.

2.4 | Winter and summer xylem embolism

Native xylem embolism was estimated by measuring the increase in hydraulic conductivity after embolism removal using a partial vacuum method (McCulloh et al., 2011). After measurement of $K_{h\text{-native}}$, the stem segments were submerged in perfusion solution (degassed 20 mM KCl) under a partial vacuum overnight (approximately 12 hr) to refill embolized tracheids. Before measurement of maximum hydraulic conductivity ($K_{h\text{-max}}$), the stem segments were inspected to confirm the absence of bubbles at their cut ends. The native percentage loss of conductivity (PLC) was calculated as

$$\mathrm{PLC} = 100\,(K_{h\text{-max}} - K_{h\text{-native}})/K_{h\text{-max}}. \quad (2)$$

2.5 | Hydraulic vulnerability curves

Stem hydraulic vulnerability curves for the plantation trees were constructed using the centrifugal force method (Alder, Pockman, Sperry, & Nuismer, 1997) on 14.2 cm long, 5–8 mm diameter stem segments from six individuals per size class. After measurement of $K_{h\text{-native}}$, the stem segments were attached to the custom-designed rotor of a high-speed centrifuge (Model 20 K, Cence Instruments, Changsha, China). Stem segments were not vacuum-infiltrated to artificially refill embolized tracheids prior to the measurements because we aimed at characterizing the hydraulic vulnerability of the functioning conduits only and also to avoid the potential impact of cavitation fatigue (Hacke, Stiller, Sperry, Pittermann, & McCulloh, 2001). Vulnerability to embolism was measured as the decrease of hydraulic conductivity in response to a stepwise increase in xylem tension (0.5, 1, 2, 2.5, 3, 3.5, 4, 4.5, 5 MPa) generated by spinning the stem segment. Spinning was held constant for 3 min at each speed level and then 3 min were allowed for equilibration under water before determination of K_h. The PLC after each spin was calculated as

$$\mathrm{PLC} = 100\,(K_{h\text{-native}} - K_h)/K_{h\text{-native}}. \quad (3)$$

2.6 | Leaf water potential

Predawn (Ψ_{pd}) and midday leaf water potential (Ψ_{md}) were measured with a pressure chamber (PMS1000; Albany, OR, USA) in trees of the five age classes at the plantation site during two consecutive sunny days in mid-July 2016. Shoot samples for Ψ_{pd} and Ψ_{md} were taken before sunrise (0400 to 0600 h) and at midday (1200 to 1400 h), respectively. For each age class, six terminal shoots each from a different individual were excised and sealed immediately in small plastic bags containing moist paper towels and kept in a cooler until water potentials were determined in the laboratory. Only the sun-exposed leaves were sampled for Ψ_{md} measurements. All samples were measured within 1 hr after excision.

2.7 | Pressure–volume relationships

Leaf pressure–volume (P–V) curves were determined using the method described by Tyree and Hammel (1972). At the plantation site, branches approximately 1 m in length were sampled from six individuals per size class at predawn and were taken to the laboratory in plastic bags containing moist paper towels. Branches were recut under water and were allowed to rehydrate for approximately 2–3 hr before terminal shoot samples were taken for determination of P–V relationships. After determination of the initial shoot fresh weight with an analytical balance (CPA 225D, Sartorius Inc., Germany), shoot weight and water potential (PMS1000) were measured periodically during slow dehydration of the shoot on the laboratory bench. Upon completion of the measurements, shoot samples were oven-dried at 70°C for 48 hr before determination of shoot dry mass. No effect of leaf

oversaturation was observed in P–V analyses (Meinzer, Woodruff, Marias, McCulloh, & Sevanto, 2014).

2.8 | Gas exchange measurements

Net CO_2 assimilation (A) and stomatal conductance (g_s) of six trees in each size class at the plantation site were measured during the summer (July to August) of 2016 using a portable photosynthesis system (Li-6400, Li-Cor Inc., Lincoln, NE, USA). The measurements were conducted on mature and fully developed sunlit leaves between 0900 and 1030 h during sunny days. Detached shoots with their base submerged in clean water were used for leaf gas exchange measurements to minimize the influence of hydraulic path-length resistance and to facilitate detection of intrinsic size-related leaf structural and physiological constraints on gas exchange (Zhang et al., 2009). Branches were cut with a pruner, immediately recut under clean water, and gas exchange measurements were made within 5 min after shoot excision. Stable readings could be taken within 2 min. Photosynthetic photon flux density and reference CO_2 in the gas exchange cuvette were held at 1,200 μmol m^{-2} s^{-1} and 400 ppm, respectively. The intrinsic water use efficiency of photosynthesis (WUE_i) was calculated as the ratio of A to g_s for each twig measured.

2.9 | Data analysis

Size-related trends in BAI, hydraulic traits (K_s, K_l, LA/SA, water potential, leaf area, wood density, and safety margin), and the relationship between Ψ_{md} and LA/SA were evaluated by linear regression analysis. The slopes of BAI against DBH relationships for the plantation and the natural forest sites were compared using analysis of covariance (ANCOVA). Differences in hydraulic traits between two sites and seasons were analysed using two-way analysis of variance (ANOVA).

3 | RESULTS

The growth pattern of *Pinus sylvestris* var. *mongolica* differed significantly between the plantation and the natural forest. Tree size of the Mongolian pine both in terms of height and DBH were significantly larger at the plantation site than that at the natural forest site in the two youngest age classes ($p < .05$, t test; Table 1). The differences between the two sites in both tree height and DBH became non-significant in the third age class (Table 1). The growth trajectories of Mongolian pine trees were significantly different at the two sites as indicated by significantly different slopes of the linear regression of BAI against DBH (Figure 1; ANCOVA). The slope of the growth trajectory was about 79% greater in the natural forest site and the increasing divergence in BAI with increasing tree size resulted in BAI being about 59–70% greater in the natural forest site in the largest DBH classes (30–35 cm). The slower growth rates found at the plantation site were consistent with the observation that trees of older age classes at the plantation site had significantly higher proportions of dead branches in their crowns than their counterparts at the natural forest site ($p < .05$; Table 1). At the plantation site, the proportion of dead branches increased from 10% to 34% across the three oldest age

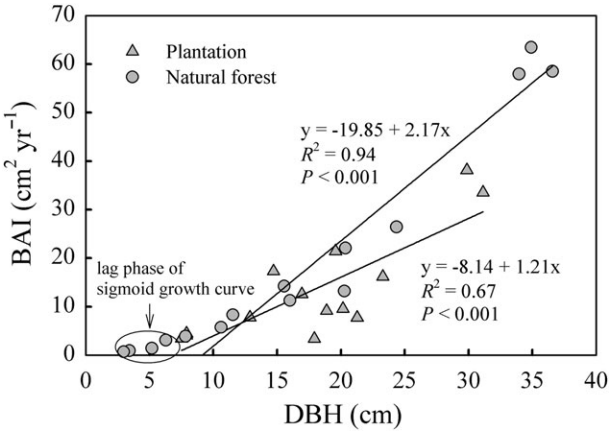

FIGURE 1 Basal area increment (BAI) in relation to stem diameter at breast height (DBH) in Mongolian pine trees at the natural forest and the plantation sites. Linear regressions were fitted to the data. Four plots with the smallest DBH at the natural forest site were excluded from the regression because they fell along the shallow portion of the sigmoid growth curve, biasing the slope of a regression fitted to the steep portion of the curve. The slopes and intercepts of the two regression lines are significantly different ($p < .05$, analysis of covariance)

classes, compared with a maximum of only 4–5% dead branches in the oldest age classes at the natural forest site (Table 1). In contrast to the size-related increase in branch dieback at the plantation site, trees at this site did not show consistent size or age-related trends in photosynthetic gas exchange parameters (A, g_s, or WUE_i) at the leaf level (Table 2).

Branch K_s decreased with increasing tree size in the plantation site, whereas no consistent trend in K_s with tree size was observed in the natural forest site (Figure 2a). With the exception of the smallest tree diameter class (4.2 cm), branch K_s was consistently higher in the natural forest site with K_s being about 31% greater in the natural forest site over a similar range of tree diameter classes for the two sites. In contrast to the size-related decline in K_s at the plantation site, K_l remained nearly constant with increasing tree size at this site (Figure 2b). The size-related variation in K_l at the natural forest site was similar to that observed for K_s, with K_l being lowest in the smallest DBH class, then increasing to a maximum value at the next larger DBH class, followed by a declining trend with further increases in DBH. Overall, K_l was substantially greater in the natural forest site (Figure 2b).

Values of PLC measured in the summer were low in all size classes in both the natural forest and the plantation sites (Figure 3a,b). In both sites, PLC values in winter, a measure of freeze–thaw induced embolism, were significantly higher than those measured in the summer in all size classes (Figure 3a,b). Most notably, the winter-time PLC values in the plantation site were two to three times greater than those of similar size classes in the natural forest site. Resistance to drought-induced hydraulic dysfunction was not significantly different among tree size classes at the plantation site with both P_{12} and P_{50} (water potentials at 12% and 50% loss of stem hydraulic conductivity, respectively) remaining nearly constant across size classes (Table 2).

TABLE 2 Physiological traits of plantation-grown *Pinus sylvestris* var. *mongolica* trees of five size classes measured during the growing season

DBH (cm)	π^{100} (MPa)	π^{0} (MPa)	A* (μmol m^{-2} s^{-1})	g_s* (mol m^{-2} s^{-1})	WUE_i (μmol mol^{-1})	P_{12} (MPa)	P_{50} (MPa)
7.77 ± 0.04 a	−2.67 ± 0.04 a	−2.81 ± 0.05 a	4.99 ± 0.43 a	0.031 ± 0.002 a	162.0 ± 6.5 a	−2.71 ± 0.07 a	−3.10 ± 0.06 a
14.84 ± 0.07 b	−2.95 ± 0.04 b	−3.12 ± 0.03 b	5.53 ± 0.37 ab	0.034 ± 0.002 ab	161.1 ± 6.5 a	−2.67 ± 0.05 a	−3.11 ± 0.05 a
18.79 ± 0.07 c	−2.50 ± 0.07 c	−2.89 ± 0.06 a	6.54 ± 0.24 bc	0.043 ± 0.004 c	160.1 ± 15.5 a	−2.56 ± 0.08 a	−3.02 ± 0.07 a
21.57 ± 0.08 d	−3.34 ± 0.08 d	−3.53 ± 0.11 c	5.71 ± 0.48 abc	0.033 ± 0.002 ad	173.5 ± 3.4 a	−2.49 ± 0.17 a	−2.92 ± 0.10 a
30.50 ± 0.20 e	−3.61 ± 0.02 e	−4.13 ± 0.06 d	6.61 ± 0.61 c	0.040 ± 0.006 bcd	169.8 ± 10.2 a	−2.64 ± 0.10 a	−3.24 ± 0.14 b

Note. Values are means ±1 *SE* (n = 6). Different letters following the values indicate significant differences between size classes at p < .05 (one-way ANOVA followed by an LSD test). DBH = diameter at breast height; π^{100} = leaf osmotic potential at full turgor; π^{0} = turgor loss point; A = maximum photosynthetic rate; g_s = stomatal conductance; WUE_i = intrinsic photosynthetic water use efficiency; P_{12} and P_{50} = xylem water potential corresponding to 12% and 50% loss of stem hydraulic conductivity. Significant differences among five size classes at p < .05 are marked by "*" (one-way ANOVA).

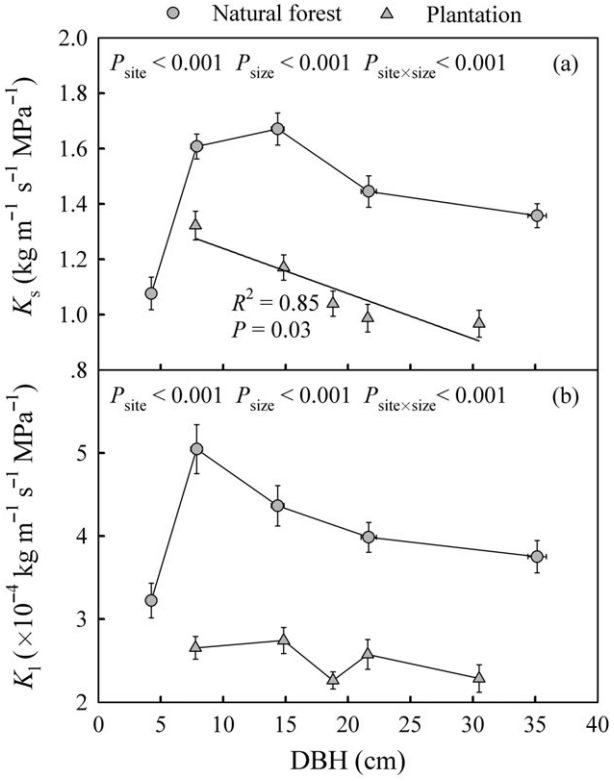

FIGURE 2 Sapwood-specific hydraulic conductivity (K_s) and leaf-specific hydraulic conductivity (K_l) of Mongolian pine trees measured in the summer for different size classes at the natural forest and the plantation sites. A linear regression was fitted to the data from the plantation site in (a). Points represent mean ± 1 *SE* (n = 20–30). Results of two-way analyses of variance are shown in each panel

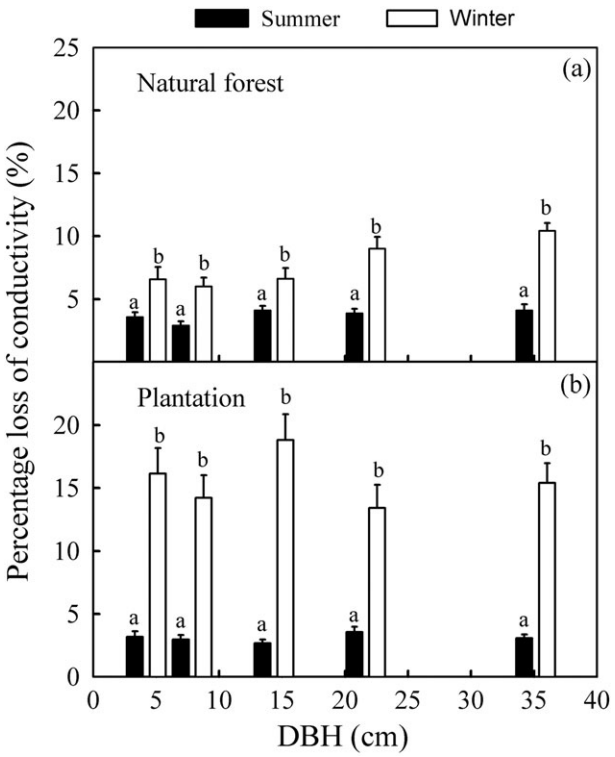

FIGURE 3 Percentage loss of hydraulic conductivity measured in Mongolian trees of different size classes during summer (black bars) and at the end of winter (white bars) for the (a) natural forest and the (b) plantation sites. Error bars show ±1 *SE* (n = 20–30). Different letters on top of error bars indicate significant differences between the two seasons within each size class at each site

There was no apparent size-related trend in branch LA/SA at the natural forest site, whereas LA/SA showed a steep linear decline from the smallest to largest DBH class at the plantation site (Figure 4a,b). For the smallest DBH class, LA/SA was substantially higher at the plantation site, then nearly equal for the two sites at medium DBH classes (14.8 to 21.6 cm), and finally at the largest DBH classes the relationship was reversed with LA/SA being roughly 1.5 times greater at the natural forest site (Figure 4a,b). Wood density showed a linear increase with increasing DBH at the plantation site, whereas it remained nearly constant at the natural forest site, except for a significant increase at the largest DBH class (p < .05; Figure 4c,d). At the plantation site, K_s showed a significant negative linear relationship with wood density across different DBH classes (the insert of Figure 4c). Trees of similar size tended to exhibit lower wood density at the plantation site than in the natural forest site.

At the plantation site, midday leaf water potential (Ψ_{md}) decreased linearly from −1.4 MPa in the smallest trees to −1.9 MPa in the largest trees (Figure 5a) resulting in parallel declines in estimated branch hydraulic safety margins (Ψ_{md}–P_{12} or Ψ_{md}–P_{50}; Figure 5b). The leaf water potential at the turgor loss point (π^{0}), calculated from the shoot pressure-volume curves, also decreased with increasing tree size, but at a faster rate than Ψ_{md} (Figure 5a). The leaf osmotic potential at full turgor (π^{100}) also decreased significantly with increasing tree size (Table 2). A strong positive relationship between LA/SA and Ψ_{md} across different DBH classes was observed at the plantation site (Figure 6).

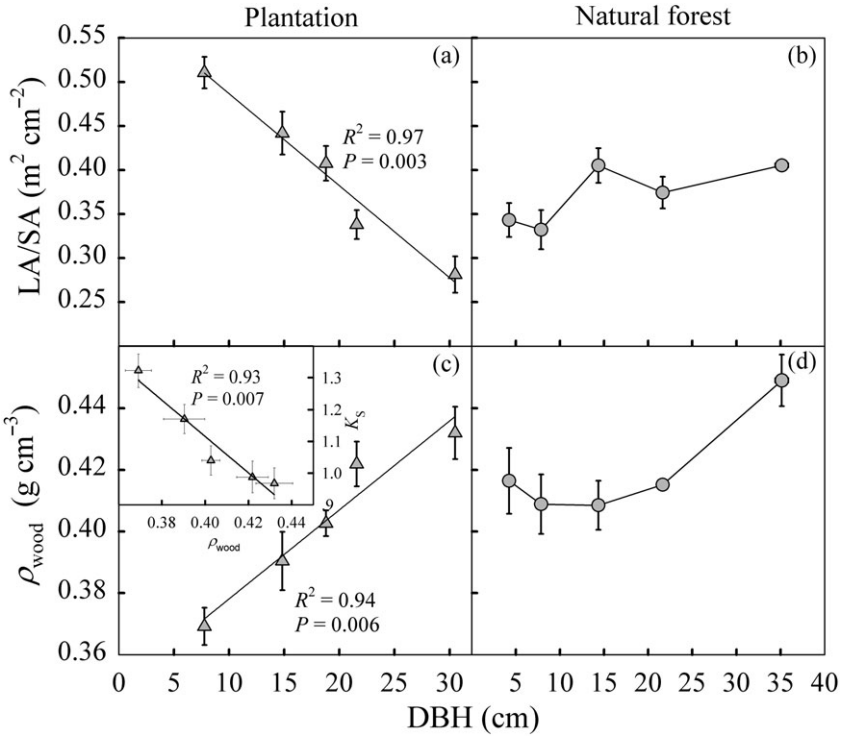

FIGURE 4 (a, b) The leaf area to sapwood area (LA/SA) ratio and (c, d) wood density (ρ_{wood}) in different size classes of Mongolian pine trees measured during the summer for the natural forest and the plantation sites. The insert in (c) shows the correlation between ρ_{wood} and sapwood-specific hydraulic conductivity (K_s). Error bars show ±1 *SE* (n = 20–30 for K_s and 12–18 for ρ_{wood}). Linear regressions were fitted to the data in (a) and (c)

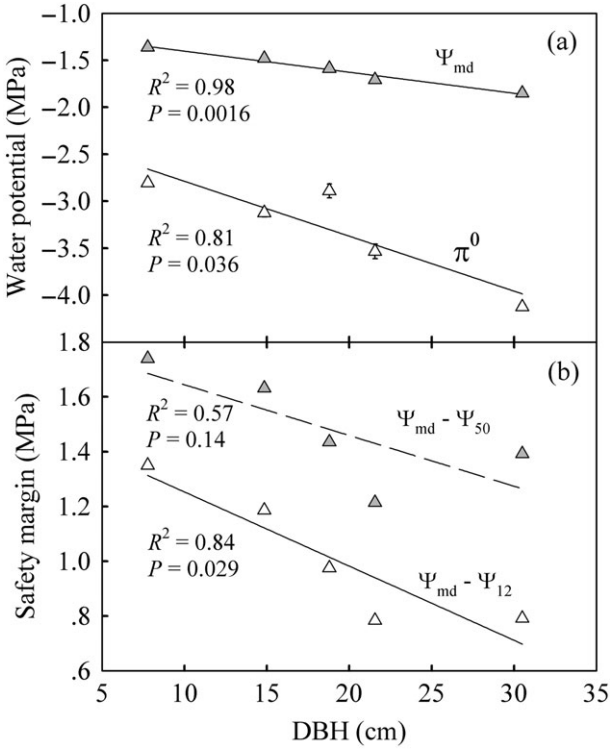

FIGURE 5 (a) Midday leaf water potential (Ψ_{md}), turgor loss point (π^0), and (b) stem hydraulic safety margins in different size classes of Mongolian pine trees measured during summer at the plantation site. Error bars in (a) show ±1 *SE* (n = 6). Linear regressions were fitted to the data

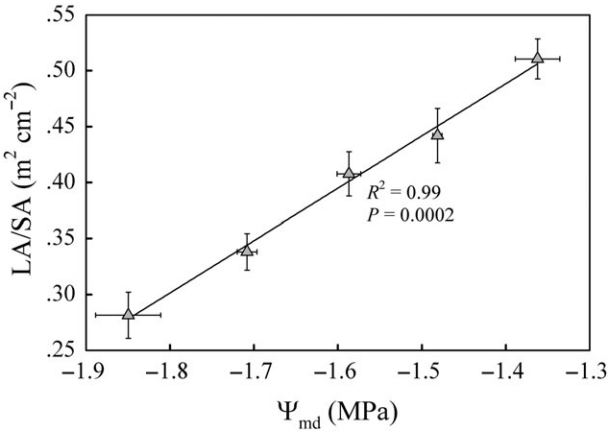

FIGURE 6 The relationship between leaf area to sapwood area ratio (LA/SA) and midday leaf water potential (Ψ_{md}) in different size classes of *Pinus sylvestris* var. *mongolica* trees measured during summer at the plantation site. Error bars show ±1 *SE* (n = 20–30 for LA/SA and n = 6 for Ψ_{md}). Linear regressions were fitted to the data

4 | DISCUSSION

Compared with the natural forest site, larger plantation-grown Mongolian pine trees showed lower stem growth rates and more crown desiccation as a result of their more challenging hydraulic environment, manifested by decreasing water potentials with increasing tree size and compensatory changes in hydraulic architecture traits. In the more water-limited habitats of the plantations, K_s decreased with increasing tree size, but K_l remained nearly constant owing to compensatory reductions in LA/SA. Although the photosynthetic rate per unit projected leaf area remained relatively constant in trees of larger size classes, the significant decrease in LA/SA with increasing tree size may have resulted in reduced efficiency of whole-tree carbon assimilation in larger trees. These changes may lead to carbon imbalances that limit the growth and even survival of larger Mongolian pine trees in the plantation site. The present study provides a potential mechanistic explanation for

the widespread dieback and mortality of this conifer species in water-limited habitats of Northern China.

4.1 | Contrasts in growth and xylem hydraulics between the two sites

Our results showed that Mongolian pine trees in the plantation site differed significantly in hydraulic architecture from those of the natural forest site with the former having substantially lower hydraulic conductivity expressed on both sapwood and leaf area bases, reflecting a relatively large phenotypic plasticity of xylem hydraulics in acclimation to different water regimes (Corcuera et al., 2011; Kavanagh, Bond, Aitken, Gartner, & Knowe, 1999). Introduction of Mongolian pine to plantations at lower latitudes implies a substantial reduction in soil water availability compared with higher latitude sites in its native range even though the annual precipitation is substantially higher in the plantation site (Table S1, Figure S1). Due to higher temperatures at lower latitudes, the plantation site has significantly higher potential evaporation, lower moisture index, and much lower snow cover in winter (Table S1). Notably, the youngest age class trees at the plantation site had significantly larger DBH than trees at the natural forest site, which is likely related to a more favourable temperature for growth and longer growing seasons when trees are introduced to lower latitudes (Sánchez-Salguero et al., 2017; Zhu et al., 2003), although nursery stock management practices favouring seedling growth at the plantation site can also play an important role. Plantation trees of the youngest age class even showed significantly greater K_s and K_l than trees at the natural forest site. However, hydraulic limitation became an increasingly important factor with the increase of tree size at the plantation site as reflected by the steep decrease of K_s with the increase of DBH, which may have exerted a strong limitation to tree performance in the older age classes. Consistent with this, when trees with DBH smaller than 7 cm were excluded from the analysis, the tree growth trajectories were significantly different between the two sites. Plantation-grown Mongolian pine trees older than 30 years often showed obvious symptoms of decline such as partial canopy dieback and periodically large-scale tree mortality, whereas no such phenomenon was observed in trees at the natural forest site even at ages older than 100 years (Song et al., 2016).

Slower growth of Mongolian pine trees at the plantation site was apparently associated with lower stem hydraulic efficiency, which is consistent with previous studies on other tree species (Fan, Zhang, Hao, Slik, & Cao, 2012; Hajek, Leuschner, Hertel, Delzon, & Schuldt, 2014). It has been found that maintaining efficient water transport and adequate water balance become limiting factors for growth and survival as trees increase in size, especially in water-limited habitats (Hember, Kurz, & Coops, 2017; Woodruff et al., 2008; Zhang et al., 2009). Our data suggest that the substantially higher degree of xylem embolism in overwintering branches of trees at the plantation site, likely due to higher frequencies of freeze–thaw cycles and lower moisture availability there (Zhu et al., 2003), may have been an important contributor to their significantly lower stem K_s than in trees of the natural forest site. Previous work has shown that reversal of winter embolism may be facilitated by absorption of water from melting snow or fog by branches and needles in late winter and early spring (Breshears et al., 2008; Hacke et al., 2015; Limm, Simonin, Bothman, & Dawson, 2009; Mayr et al., 2014). Winter embolism reversal is likely to be impaired by the more intermittent snow cover, lower air humidity, and higher winter evaporative demand at the plantation site (Burgess & Dawson, 2004; Eller, Lima, & Oliveira, 2013; Limm et al., 2009), which could result in cumulative high xylem dysfunction and winter branch desiccation (Mayr et al., 2014; Sparks et al., 2001). Winter desiccation is such an important factor affecting the performance of Mongolian pine trees at the plantation site that seedlings younger than 3 years old almost never survive a winter if they are not artificially buried in the sand to retain moisture and then uncovered in the following spring (Yan & Long, 2008; Zhao et al., 2015).

4.2 | Compensatory adjustments to water stress with increasing tree size in plantations

To deal with their less efficient hydraulic system, trees at the plantation site seemed to compensate for increasing water stress by adjusting their hydraulic architecture as observed in other tree species (Pfautsch et al., 2016; Zhang et al., 2009). Decreased LA/SA with increasing tree size in the plantations is likely a homeostatic mechanism that partially compensates for decreases in K_s and contributes to the maintenance of a nearly constant K_l among size classes (Figure 2b). The maintenance of relatively stable photosynthetic gas exchange rates with increasing tree size, despite the reduction in xylem water transport efficiency, indicated that this branch-level compensatory adjustment in the water supply and demand relationship can at least partially mitigate the hydraulic limitation to leaf gas exchange in larger trees (Becker, Meinzer, & Wullschleger, 2000; Woodruff et al., 2004). A plausible mechanism responsible for a reduction in LA/SA might be that lower turgor at more negative water potentials might have led to reduced leaf expansion in the larger Mongolian pine tree size classes because turgor plays a dominant role in regulating leaf expansion particularly when the external osmotic environment changes under water stress (Ryan et al., 2006; Woodruff et al., 2004).

Consistent with the decrease in K_s with increasing tree size, adjustments in leaf water relations also occurred as reflected by lower π^0 and π^{100} values in trees of larger size classes at the plantation site. The size-related osmotic adjustment observed in the present study appears to be analogous to that observed in other woody species across gradients of increasing aridity (Hao et al., 2008; Hao, Sack, Wang, Cao, & Goldstein, 2010; Pfautsch et al., 2016). Although the plantation trees in our study spanned a relatively narrow range of height, our results are consistent with the finding that cumulative hydraulic resistances associated with longer water transport pathways cause greater water stress in crowns of taller trees, which are also potentially exposed to higher evaporative demand (Barnard & Ryan, 2003; Ryan et al., 2006). In our study, π^0 decreased more rapidly than Ψ_{md} with increasing tree size, suggesting an increase in the "turgor safety margin" (Figure 5a). However, the apparent greater "turgor safety margin" in larger trees was associated with lower LA/SA and thus likely lower leaf expansion rates, implying that the more negative turgor loss points measured in mature leaves of larger trees may not

necessarily apply to their expanding leaves (Meinzer et al., 2008; Woodruff et al., 2004).

4.3 | Physiological constraints on larger trees in plantations

Higher degrees of branch dieback and a syndrome of greater water stress in the upper crown of larger Mongolian pine trees of the plantation site are in accordance with the widely observed decline in productivity and increased risk of mortality with increasing tree size (Martínez-Vilalta, Vanderklein, & Mencucini, 2007; Mencuccini et al., 2005; Ryan et al., 1997). Although compensatory adjustments in hydraulic architecture with increasing tree size can mitigate the influence of higher hydraulic resistance in larger trees to a certain degree, this adjustment may be unsustainable in terms of long-term carbon balance at the whole-plant level, eventually leading to limitation on tree growth or even tree death in chronically water-limited environments (Sperry, Meinzer, & McCulloh, 2008; Zhang et al., 2009). Increasing evidence suggests that carbon starvation may be another important cause for tree dieback or death in water-stressed environments that should not be viewed in isolation from hydraulic failure (McDowell et al., 2011; Rodríguez-Calcerrada et al., 2017). Even if the net photosynthetic rate on a unit leaf area basis remains relatively constant with increasing tree size, substantial reductions in leaf area necessary for maintaining adequate water balance would unavoidably exert a strong negative influence on carbon acquisition at the whole plant level that may eventually result in carbon imbalance in water-limited environments (Bennett et al., 2015; Zhang et al., 2009). The observation that plantation trees older than 30 years often show substantial numbers of dead branches and have considerably smaller crowns than natural forest trees of similar DBH, strongly suggests that carbon imbalance may also involve in causing mortality of plantation-grown Mongolian pine trees in water-limited environments.

Under the plantation growth conditions, larger trees appeared to operate with a significantly reduced hydraulic safety margin that may put them at greater risks of dieback or mortality due to hydraulic failure. This is in line with findings from recent studies showing that larger trees are dying in higher frequencies than smaller ones when facing severe drought stress (Bennett et al., 2015; Ryan, 2015). Nevertheless, the stem P_{50} value, considered to represent the mortality threshold for gymnosperms (Brodribb & Cochard, 2009; Choat et al., 2012), was considerably more negative than midday water potentials in trees at the plantation site even in the largest size class, resulting in a relatively large hydraulic safety margin, consistent with a strategy of functional homeostasis in terms of water relations in pines (Choat et al., 2012; Magnani et al., 2002; Meinzer et al., 2014). However, these values should be interpreted within an absolute minimum water potential experienced by plants in the field. Trees may experience much lower water potentials that push them past their hydraulic tipping point under decadal extreme drought stresses that are not normally experienced in a given growing season (Maherali, Pockman, & Jackson, 2004; Zweifel & Zeugin, 2008). Under these extreme conditions, the significantly reduced hydraulic safety margin in larger plantation-grown Mongolian pine trees would have likely contributed to their greater frequencies of mortality (Delzon & Cochard, 2014). Moreover, higher wood density in trees of larger size classes may reduce the wood hydraulic capacitance, lowering its ability to buffer fluctuations in water deficits (Meinzer et al., 2008; Scholz et al., 2007; Zhang et al., 2009), potentially contributing to greater risk of mortality under extreme drought as suggested by interspecific comparative studies on species of varying wood density (Hoffmann et al., 2011).

4.4 | Concluding remarks

Results of our comparative study between the two sites and across different tree size classes indicate that greater hydraulic limitation with increasing tree size may exert an increasingly stronger limitation on performance of Mongolian pine trees in the more water-limited environments of plantations. The significantly reduced hydraulic safety margins in larger size classes of Mongolian pine trees in the plantations can potentially put them at greater risk of dieback or mortality due to hydraulic failure, especially during extreme climate variations. Although compensatory adjustments in branch hydraulic architecture and leaf level water relations appeared to be effective in mitigating the effect of increased water stress in the upper crown, substantial reductions in leaf area may likely increase the risk of carbon imbalances at the whole-plant level that can cause tree decline in the long run. Our results provide a potential mechanistic explanation for the widespread decline of Mongolian pine plantations in Northern China, although other mechanisms not captured in the current dataset, such as below-ground hydraulic decline (Dawson, 1996; Martínez-Vilalta, Korakaki, Vanderklein, & Mencuccini, 2007), may also be important especially to trees growing in sandy soils.

Due to the lower soil moisture availability at the plantation site, management strategies that reduce water consumption at the stand level, such as reducing the planting density and tree thinning, would contribute to the mitigation of plantation decline. Although planted trees may survive for a considerable period of time, their eventual decline and mortality may become unavoidable due to water limitation associated with increasing tree size. It is important to note that the stable climax vegetation at the plantation site before land degradation was known to be Savanna-like grassland with sparse trees.

ACKNOWLEDGMENTS

We thank Na Li, Lin Chao, Lidong Fang, and Cunyang Niu for field assistances. This work was supported by the National Natural Science Foundation of China (31722013, 31500222), the National Key Research and Development Program of China (2016YFA0600803), the Project of Natural Science and Technology of Liaoning Province of China (20170540899), Key Research Project from the Bureau of Frontier Science and Education Chinese Academy of Sciences (QYZDJ-SSW-DQC027), and the Hundred-Talents Program from the Chinese Academy of Sciences. The authors declare no conflict of interests.

ORCID

Frederick C. Meinzer http://orcid.org/0000-0003-2387-2031
Guang-You Hao http://orcid.org/0000-0002-6003-7003

REFERENCES

Adams, H. D., Guardiola-Claramonte, M., Barron-Gafford, G. A., Villegas, J. C., Breshears, D. D., Zou, C. B., … Huxman, T. E. (2009). Temperature

sensitivity of drought-induced tree mortality portends increased regional die-off under globle-change-type drought. *Proceedings of the National Academy of Sciences*, *106*, 7063–7066.

Alder, N. N., Pockman, W. T., Sperry, J. S., & Nuismer, S. (1997). Use of centrifugal force in the study of xylem cavitation. *Journal of Experimental Botany*, *48*, 665–674.

Allen, C. D., Macalady, A. K., Chenchouni, H., Bachelet, D., McDowell, N., Vennetier, M., … Cobb, N. (2010). A global overview of drought and heat-induced tree mortality reveals emerging climate change risks for forests. *Forest Ecology and Management*, *259*, 660–684.

Anderegg, W. R. L., Berry, J. A., Smith, D. D., Sperry, J. S., Anderegg, L. D. L., & Field, C. B. (2012). The roles of hydraulic and carbon stress in a widespread climate-induced forest die-off. *Proceedings of the National Academy of Sciences*, *109*, 233–237.

Balducci, L., Deslauriers, A., Giovannelli, A., Rossi, S., & Rathgeber, C. B. K. (2013). Effects of temperature and water deficit on cambial activity and woody ring features in *Picea mariana* sapling. *Tree Physiology*, *33*, 1006–1017.

Barnard, H. R., & Ryan, M. G. (2003). A test of the hydraulic limitation hypothesis in fast-growing *Eucalyptus saligna*. *Plant, Cell and Environment*, *26*, 1235–1245.

Becker, P., Meinzer, F. C., & Wullschleger, S. D. (2000). Hydraulic limitation of tree height: A critique. *Functional Ecology*, *14*, 4–11.

Bennett, A. C., McDowell, N. G., Allen, C. D., & Anderson-Teixeira, K. J. (2015). Larger trees suffer most during drought in forests worldwide. *Nature Plants*, *1*, 1–5.

Breshears, D. D., McDowell, N. G., Goddard, K. L., Dayem, K. E., Martens, S. N., Meyer, C. W., & Brown, K. M. (2008). Foliar absorption of intercepted rainfall improves woody plant water status most during drought. *Ecology*, *89*, 41–47.

Brodribb, T. J., & Cochard, H. (2009). Hydraulic failure defines the recovery and point of death in water-stressed conifers. *Plant Physiology*, *149*, 575–584.

Burgess, S. S. O., & Dawson, T. E. (2004). The contribution of fog to the water relations of *Sequoia sempervirens* (D. Don): Foliar uptake and prevention of dehydration. *Plant, Cell and Environment*, *27*, 1023–1034.

Charrier, G., Charra-Vaskou, K., Kasuga, J., Cochard, H., Mayr, S., & Améglio, T. (2014). Freeze-thaw stress: Effects of temperature on hydraulic conductivity and ultrasonic activity in ten woody angiosperms. *Plant Physiology*, *164*, 992–998.

Choat, B., Jansen, S., Brodribb, T. J., Cochard, H., Delzon, S., Bhaskar, R., … Zanne, A. E. (2012). Global convergence in the vulnerability of forests to drought. *Nature*, *491*, 752–756.

Cochard, H., & Tyree, M. T. (1990). Xylem dysfunction in *Quercus*: Vessel sizes, tyloses, cavitation and seasonal changes in embolism. *Tree Physiology*, *6*, 393–407.

Corcuera, L., Cochard, H., Pelegrín, E. G., & Notivol, E. (2011). Phenotypic plasticity in mesic populations of *Pinus pinaster* improves resistance to xylem embolism (P_{50}) under severe drought. *Trees*, *25*, 1033–1042.

Davis, S. D., Ewers, F. W., Sperry, J. S., Portwood, K. A., Crocker, M. C., & Adams, G. C. (2002). Shoot dieback during prolonged drought in *Ceanothus* (Rhamnaceae) chaparral of California: A possible case of hydraulic failure. *American Journal of Botany*, *89*, 820–828.

Dawson, T. E. (1996). Determing water use by trees and forests from isotopic, energy balance and transpiration analyses: The role of tree size and hydraulic lift. *Tree Physiology*, *16*, 263–272.

Delzon, S., & Cochard, H. (2014). Recent advances in tree hydraulics highlight the ecological significance of the hydraulic safety margin. *New Phytologist*, *203*, 355–358.

Domec, J. C., Lachenbruch, B., Meinzer, F. C., Woodruff, D. R., Warren, J. M., & McCulloh, K. A. (2008). Maximum height in a conifer is associated with conflicting requirements for xylem design. *Proceedings of the National Academy of Sciences*, *105*, 12069–12074.

Eller, C. B., Lima, A. L., & Oliveira, R. S. (2013). Foliar uptake of fog water and transport belowground alleviates drought effects in the cloud forest tree species, *Drimys brasiliensis* (Winteraceae). *New Phytologist*, *199*, 151–162.

Fan, Z. X., Zhang, S. B., Hao, G. Y., Slik, F., & Cao, K. F. (2012). Hydraulic conductivity traits predict growth rates and adult stature of 40 Asian tropical tree species better than wood density. *Journal of Ecology*, *100*, 732–741.

Hacke, U. G., Lachenbruch, B., Pittermann, J., Mayr, S., Domec, J. C., & Schulte, P. J. (2015). The hydraulic architecture of conifers. In U. Hacke (Ed.), *Functional and ecological xylem anatomy* (pp. 56–58). Switzerland: Springer.

Hacke, U. G., Stiller, V., Sperry, J. S., Pittermann, J., & McCulloh, K. A. (2001). Cavitation fatigue. Embolism and refilling cycles can weaken the cavitation resistance of xylem. *Plant Physiology*, *125*, 779–786.

Hajek, P., Leuschner, C., Hertel, D., Delzon, S., & Schuldt, B. (2014). Trade-offs between xylem hydraulic properties, wood anatomy and yield in *Populus*. *Tree Physiology*, *34*, 744–756.

Hao, G. Y., Hoffmann, W. A., Scholz, F. G., Bucci, S. J., Meinzer, F. C., Franco, A. C., … Goldstein, G. (2008). Stem and leaf hydraulics of congeneric tree species from adjacent tropical savanna and forest ecosystems. *Oecologia*, *155*, 405–415.

Hao, G. Y., Sack, L., Wang, A. Y., Cao, K. F., & Goldstein, G. (2010). Differentiation of leaf water flux and drought tolerance traits in hemiepiphytic and non-hemiepiphytic *Ficus* tree species. *Functional Ecology*, *24*, 731–740.

Hartmann, H. (2011). Will a 385 million year-struggle for light become a struggle for water and for carbon?—How trees may cope with more frequent climate change-type drought events. *Global Change Biology*, *17*, 642–655.

Hember, R. A., Kurz, W. A., & Coops, N. C. (2017). Relationships between individual-tree mortality and water-balance variables indicate positive trends in water stress-induced tree mortality across North America. *Global Change Biology*, *23*, 1691–1710.

Hoffmann, W. A., Marchin, R. M., Abit, P., & Lau, O. L. (2011). Hydraulic failure and tree dieback are associated with high wood density in a temperate forest under extreme drought. *Global Change Biology*, *17*, 2731–2742.

Jiang, F. Q., Zeng, D. H., & Zhu, J. J. (1997). Fundamentals and technical strategy for sand-fixation forest management. *Chinese Journal of Desert Research*, *17*, 250–254.

Jiao, S. R. (2001). Report on the causes of the early decline of *Pinus sylvestris* var. *mongolica* shelterbelt and its preventative and control measures in Zhanggutai of Liaoning province. *Scientia Silvae Sinicae*, *37*, 131–138.

Kang, H. Z., Zhu, J. J., Li, Z. H., & Xu, M. L. (2004). Natural distribution of *Pinus sylvestris* var. *mongolica* on sandy land and its cultivation as an exotic species. *Chinese Journal of Ecology*, *23*, 134–139.

Kavanagh, K. L., Bond, B. J., Aitken, S. N., Gartner, B. L., & Knowe, S. (1999). Shoot and root vulnerability to xylem cavitation in four populations of *Douglas-fir* seedlings. *Tree Physiology*, *19*, 31–37.

Koch, G. W., Sillet, S. C., Jennings, G. W., & Davis, S. D. (2004). The limits of tree height. *Nature*, *428*, 851–854.

Langan, S. J., Ewers, F. W., & Davis, S. D. (1997). Xylem dysfunction caused by water stress and freezing in two species of co-occurring chaparral shrubs. *Plant, Cell and Environment*, *20*, 425–437.

Limm, E. B., Simonin, K. A., Bothman, A. G., & Dawson, T. E. (2009). Foliar water uptake: A common water acquisition strategy for plants of the redwood forest. *Oecologia*, *161*, 449–459.

Magnani, F., Grace, J., & Borghetti, M. (2002). Adjustment of tree structure in response to the environment under hydraulic constraints. *Functional Ecology*, *16*, 385–393.

Maherali, H., Pockman, W. T., & Jackson, R. B. (2004). Adaptive variation in the vulnerability of woody plants to xylem cavitation. *Ecology*, *85*, 2184–2199.

Martínez-Vilalta, J., Korakaki, E., Vanderklein, D., & Mencucini, M. (2007). Below-ground hydraulic conductance is a function of environmental

conditions and tree size in Scots pine. *Functional Ecology*, *21*, 1072–1083.

Martínez-Vilalta, J., López, B. C., Loepfe, L., & Lloret, F. (2012). Stand- and tree-level determinants of the drought response of Scots pine radial growth. *Oecologia*, *168*, 877–888.

Martínez-Vilalta, J., & Piñol, J. (2002). Drought-induced mortality and hydraulic architecture in pine populations of the NE Iberian Peninsula. *Forest Ecology and Management*, *161*, 247–256.

Martínez-Vilalta, J., Vanderklein, D., & Mencuccini, M. (2007). Tree height and age-related deline in growth in Scots pine (*Pinus sylvestris* L.). *Oecologia*, *150*, 529–544.

Mayr, S., Schmid, P., Laur, J., Rosner, S., Charra-Vaskou, K., Dämon, B., & Hacke, U. G. (2014). Uptake of water via branches helps timberline conifers refill embolized xylem in late winter. *Plant Physiology*, *164*, 1731–1740.

McCulloh, K. A., Johnson, D. M., Meinzer, F. C., & Lachenbruch, B. (2011). An annual pattern of native embolism in upper branches of four tall conifer species. *American Journal of Botany*, *98*, 1007–1015.

McDowell, N. G., & Allen, C. D. (2015). Darcy's law predicts widespread forest mortality under climate warming. *Nature Climate Change*, *5*, 669–672.

McDowell, N. G., Beerling, D. J., Breshears, D. D., Fisher, R. A., Raffa, K. F., & Stitt, M. (2011). The interdependence of mechanisms underlying climate-driven vegetation mortality. *Trends in Ecology and Evolution*, *26*, 523–532.

McDowell, N. G., Pockman, W. T., Allen, C. D., Breshears, D. D., Cobb, N., Kolb, T., … Yepez, E. A. (2008). Mechanisms of plant survival and mortality during drought: Why do some plants survive while others succumb to drought? *New Phytologist*, *178*, 719–739.

Meinzer, F. C., Campanello, P. I., Domec, J. C., Gatti, M. G., Goldstein, G., Villalobos-Vega, R., & Woodruff, D. R. (2008). Constraints on physiological function associated with branch architecture and wood density in tropical forest trees. *Tree Physiology*, *28*, 1609–1617.

Meinzer, F. C., Woodruff, D. R., Marias, D. E., McCulloh, K. A., & Sevanto, S. (2014). Dynamics of leaf water relations components in co-occurring iso- and anisohydric conifer species. *Plant, Cell and Environment*, *37*, 2577–2586.

Mencuccini, M., Martínez-Vilalta, J., Vanderklein, D., Hamid, H. A., Korakaki, E., Lee, S., & Michiels, B. (2005). Size-mediated ageing reduces vigour in trees. *Ecology Letters*, *8*, 1183–1190.

Nardini, A., Battistuzzo, M., & Savi, T. (2013). Shoot desiccation and hydraulic failure in temperate woody angiosperms during an extreme summer drought. *New Phytologist*, *200*, 322–329.

O' Grady, A. P., Mitchell, P. J., Pinkard, E. A., & Tissue, D. T. (2013). Thirsty roots and hungry leaves: Unravelling the role roles of carbon and water dynamics in tree mortality. *New Phytologist*, *200*, 294–297.

Pfautsch, S., Harbusch, M., Wesolowski, A., Smith, R., Macfarlane, C., Tjoelker, M. G., … Adams, M. A. (2016). Climate determines vascular traits in the ecologically diverse genus *Eucalyptus*. *Ecology Letters*, *19*, 240–248.

Rodríguez-Calcerrada, J., Li, M., López, R., Cano, F. J., Oleksyn, J., Atkin, O. K., … Gil, L. (2017). Drought-induced shoot dieback starts with massive root xylem embolism and variable depletion of nonstructural carbohydrates in seedlings of two tree species. *New Phytologist*, *213*, 597–610.

Ryan, M. G. (2015). Large trees losing out to drought. *Nature*, *1*, 15150.

Ryan, M. G., Binkley, D., & Fownes, J. H. (1997). Age-related decline in forest productivity: Pattern and process. *Advances in Ecological Research*, *27*, 213–262.

Ryan, M. G., Phillips, N., & Bond, B. J. (2006). The hydraulic limitation hypothesis revisited. *Plant, Cell and Environment*, *29*, 367–381.

Sánchez-Salguero, R., Camarero, J. J., Gutiérrez, E., Rouco, F. G., Gazol, A., Sangüesa-Barreda, G., … Seftigen, K. (2017). Assessing forest vulnerability to climate warming using a process-based model of tree growth: Bad prospects for rear-edges. *Global Change Biology*, *23*, 2705–2719.

Scholz, F. G., Bucci, S. J., Goldstein, G., Meinzer, F. C., Franco, A. C., & Miralles-Wilhelm, F. (2007). Biophysical properties and functional significance of stem water storage tissues in Neotropical savanna trees. *Plant, Cell and Environment*, *30*, 236–248.

Schuldt, B., Knutzen, F., Delzon, S., Jansen, S., Müller-Haubold, H., Burlett, R., … Leuschner, C. (2016). How adaptable is the hydraulic system of European beech in the face of climate change-related precipitation reduction? *New Phytologist*, *210*, 443–458.

Sevanto, S., McDowell, N. G., Dickman, L. T., Pangle, R., & Pockman, W. T. (2014). How do trees die? A test of the hydraulic failure and carbon starvation hypotheses. *Plant, Cell and Environment*, *37*, 153–161.

Song, L. N., Zhu, J. J., Li, M. C., & Zhang, J. X. (2016). Water use patterns of *Pinus sylvestris* var. *mongolica* trees of different ages in semiarid sandy lands of Northeast China. *Environmental and Experimental Botany*, *129*, 94–107.

Song, L. N., Zhu, J. J., Yan, Q. L., Li, M. C., & Yu, G. Q. (2015). Comparison of intrinsic water use efficiency between different aged *Pinus sylvestris* var. *mongolica* windbreaks in semiarid sandy land of northern China. *Agroforestry Systems*, *89*, 477–489.

Sparks, J. P., Campbell, G. S., & Black, R. A. (2001). Water content, hydraulic conductivity, and ice formation in winter stems of *Pinus contorta*: A TDR case study. *Oecologia*, *127*, 468–475.

Sperry, J. S., Meinzer, F. C., & McCulloh, K. A. (2008). Safety and efficiency conflicts in hydraulic architecture: Scaling from tissues to trees. *Plant, Cell and Environment*, *31*, 632–645.

Sperry, J. S., & Sullivan, J. E. M. (1992). Xylem embolism in response to freeze-thaw cycles and water stress in ring-porous, diffuse-porous and conifer species. *Plant Physiology*, *100*, 605–613.

Tyree, M. T., & Hammel, H. T. (1972). The measurement of the turgor pressure and the water relations of plants by the pressure-bomb technique. *Journal of Experimental Botany*, *23*, 267–282.

Wong, C. M., & Daniels, L. D. (2016). Novel forest decline triggered by multiple interactions among climate, an introduced pathogen and bark beetles. *Global Change Biology*, *23*, 1926–1941.

Woodruff, D. R., Bond, B. J., & Meinzer, F. C. (2004). Does turgor limit growth in tall trees? *Plant, Cell and Environment*, *27*, 229–236.

Woodruff, D. R., Meinzer, F. C., & Lachenbruch, B. (2008). Height-related trends in leaf xylem anatomy and shoot hydraulic characteristics in a tall conifer: Safety versus efficiency in water transport. *New Phytologist*, *180*, 90–99.

Xu, C., McDowell, N. G., Sevanto, S., & Fisher, R. A. (2013). Our limited ability to predict vegetation dynamics under water stress. *New Phytologist*, *200*, 298–300.

Yan, X. L., & Long, S. H. (2008). Experiment on overwintering management of *Pinus sylvestris* var. *mongolica* seedlings. *Chinese Journal of Hebei Forestry Science and Technology*, *4*, 20–21.

Zeng, D. H., Jiang, F. Q., Fan, Z. P., & Zhu, J. J. (1996). Stability of Mongolian pine plantations on sandy land. *Chinese Journal of Applied Ecology*, *7*, 337–343.

Zhang, Y. J., Meinzer, F. C., Hao, G. Y., Scholz, F. G., Bucci, S. J., Takahashi, F. S. C., … Goldstein, G. (2009). Size-dependent mortality in a Neotropical savanna tree: The role of height-related adjustments in hydraulic architecture and carbon allocation. *Plant, Cell and Environment*, *32*, 1456–1466.

Zhao, H. L., Li, J., Zhou, R. L., Qu, H., Yun, J. Y., & Pan, C. C. (2015). Effects of sand burial on growth properties of *Pinus sylvestris* var. *mongolica*. *Chinese Journal of Desert Research*, *35*, 60–65.

Zheng, X., Zhu, J. J., Yan, Q. L., & Song, L. N. (2012). Effects of land use changes on groundwater table and the decline of *Pinus sylvestris* var. *mongolica* plantations in the Horqin Sandy Land, Northeast China. *Agricultural Water Management*, *109*, 94–106.

Zhu, J. J., Fan, Z. P., Zeng, D. H., Jiang, F. Q., & Matsuzaki, T. (2003). Comparison of stand structure and growth between artificial and natural forests of *Pinus sylvestris* var. *mongolica* on sandy land. *Journal of Forest Research*, *14*, 103–111.

Zweifel, R., & Zeugin, F. (2008). Ultrasonic acoustic emissions in drought-stressed trees—More than signals from caviation? *New Phytologist*, *179*, 1070–1079.

SUPPORTING INFORMATION

Additional Supporting Information may be found online in the supporting information tab for this article.

How to cite this article: Liu Y-Y, Wang A-Y, An Y-N, et al. Hydraulics play an important role in causing low growth rate and dieback of aging *Pinus sylvestris* var. *mongolica* trees in plantations of Northeast China. *Plant Cell Environ*. 2018;1–12. https://doi.org/10.1111/pce.13160